International Journal for Research in Applied Science & Engineering Technology (IJRASET)

DigSILENT Modeling of Power Electronic Converters for Distributed Generation systems

VenkateswaraReddy .G[1], Chandrakala. B[2]

M. Tech scholar, Department of EEE LakkiReddy BaliReddy College of engineering, Vijayawada, India.

Assistant professor, Department of EEE, LakkiReddy BaliReddy College of engineering, Vijayawada, India.

Abstract: In this paper with increasing levels of small-scale distributed generation (DG) systems connecting into the electrical grid, there is a growing awareness of potentially adverse interactions between these systems and the grid because of their differing responses to steady state and transient network events. To study the simulation models of both the grid network and the DG inverter systems that are efficiently explain to their real world physical system behaviors. In this power inverter model developed in the DigSILENT power factory. And also explain the inverter operation up to the PWM switching frequency, but is still computationally viable for use with larger scale system studies.

Index Terms: - DigSILENT power factory, power inverter, distributed generation system.

I.   INTRODUCTION

The levels of Distributed Generation (DG) injecting into the electrical distribution system network at the end-user connection point, have been steadied the past few years [1-3] these injection levels is an increasing relation about the potential impact of distributed generation systems on the control and operation of their associated power system network. Hence the control structures of these systems need to be considered within the framework of their associated power system network [4, 5]. Typically, this is done by incorporating a simplified "averaged" DG inverter model into a standard power system analysis package.

Two of the most significant concerns for large scale DG penetrations are their effect on network feeder voltage profiles and on distribution grid fault protection responses.

Ref [6] investigates the voltage profile issue, reporting on the impact of high levels of PV penetration in residential areas taking into account transformer and feeder impedances, and levels of penetration. Ref [7] explores the feeder protection and operation issue, looking at the case of high residential PV penetration on a distribution feeder protection system. Such references identify significant voltage profile and system protection influences caused by high PV penetration levels, with differing levels of impact depending on whether a few large size DG units or many small-size PV systems are installed [8]. The further impact of energy storage devices associated with DG units is discussed in [9], and suggests that the network transient stability can actually be improved using energy storage devices such as batteries and ultra-capacitors.

Another significant issue for increasing penetration levels of DG systems is grid harmonic distortion which is discussed in [10-15]. Ref [10] proposes a harmonic analysis method based on inverter output impedance if the switching frequency is much higher than the frequency of interest, suggesting that limitations should be specified for impedances that are used in DG inverter design. Other approaches have also been proposed [11, 15]to compensate for DG system harmonics.

Many of these studies model the DG inverter system as an average equivalent voltage source behind reactance, similar to a conventional rotating machine. Some include a simplified closed loop regulation system for the inverter, but almost all ignore what are known from inverter studies to be important second order effects, such as modulation harmonics, sampling delays, and closed loop gain settings. Hence the validity of their modelling in terms of representing the response of a real physical inverter system is at best uncertain.

 This paper addresses this issue, by developing a detailed model of a DG inverter system within the power system

Analysis package DigSILENT [16]. The model controls a DigSILENT switched inverter block using a detailed leading edge closed loop current regulator that is based on an existing inverter model developed previously in PSIM and then experimentally validated

International Journal for Research in Applied Science & Engineering Technology (IJRASET)

[17]. The outcome provides the capability to combine a validated accurate inverter model with a detailed model of a grid network, to efficiently explore the overall system and multiple DG inverter responses to a variety of network loading conditions and transient events.
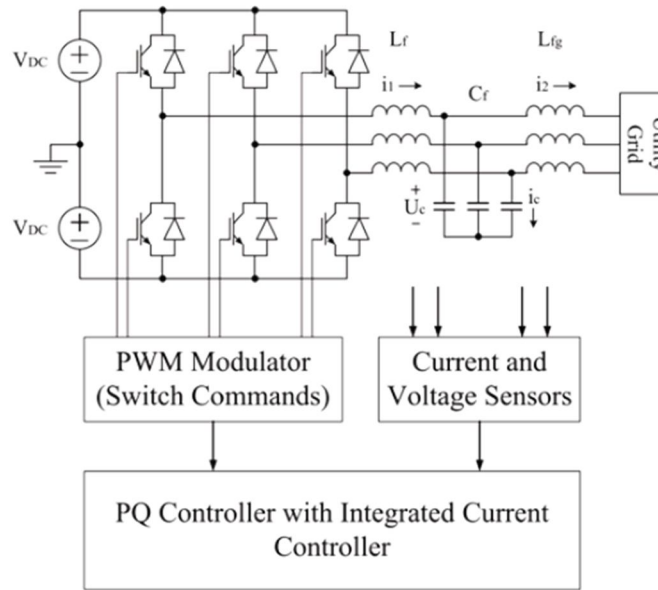
II.   3-PHASE DG CONVERTER MODEL

Fig.1 Structure of a three phase VSI used for a DG system.

Fig. 1 shows the structure of a typical three phase voltage source inverter used to connect a DG system to the electrical network. It consists of a center tapped dc voltage source (the DG energy source) which supplies a switched three phase bridge converter. The converter outputs connect to the utility network via an LCL filter at the point-of-common-coupling. The converter is controlled by a high level PQ control algorithm that calculates the required currents to inject commanded levels of real and reactive power for given measured grid voltages. These commanded currents are then processed by a lower level current regulator, to create commanded average output voltages for each phase leg that feed through the Pulse Width Modulator to generate the phase leg switching commands. To adequately simulate the dynamic response of such a DG inverter system, it is important to properly represent all three of these converter control systems. For control purposes it is convenient to transform the converter variables into a synchronous rotating dq reference frame using the following abc to dq transformation.

$$[I_{dqo}] = \sqrt{\frac{2}{3}} \begin{bmatrix} cos(\theta) & cos\left(\theta - \frac{2\pi}{3}\right) & cos\left(\theta + \frac{2\pi}{3}\right) \\ -\sin(\theta) & -sin\left(\theta - \frac{2\pi}{3}\right) & -sin\left(\theta + \frac{2\pi}{3}\right) \\ \frac{\sqrt{2}}{2} & \frac{\sqrt{2}}{2} & \frac{\sqrt{2}}{2} \end{bmatrix} \begin{bmatrix} I_a \\ I_b \\ I_c \end{bmatrix}$$

.... (1)

Where I_{dq0} denotes the current elements in d, q and 0 axis.

International Journal for Research in Applied Science & Engineering Technology (IJRASET)
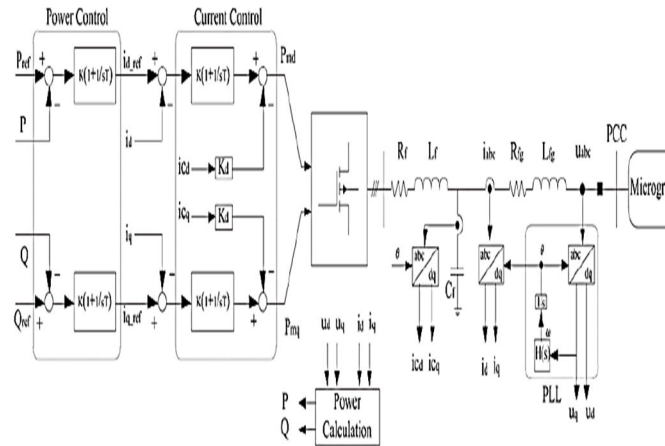

Fig. 2 Schematic diagram of the three-phase DG unit and its corresponding control architecture.

This transformation allows simple PI structures to be used for the power and current controllers, since they operate on "dc" converter variables in the synchronous frame and hence can achieve zero steady-state error because of the infinite DC gain of a PI regulator. Furthermore, only two regulator structures are required, in the d and q axes only, because the floating neutral connection of the utility grid means that the three phase currents must always sum to zero, and hence there is no fundamental zero-sequence current flowing through the inverter system.

III.   CONTROL SCHEME FOR THREE-PHASE DG SYSTEM

A.   Primary Control Structure

The main objective of the controller is to regulate the real and reactive power that is injected into the grid system, using a closed loop current regulator that drives a high frequency PWM switching controller. The detailed structure of the primary control system that achieves this objective is shown in Fig. 2.

The target real and reactive power commands P_{ref} and Q_{ref} that feed into the system are either commanded from   a remote controller, or are set to constant values for a desired level of PQ control. As indicated in Fig. 2, i_{abc} and U_{abc} are measured in the abc frame, and then converted to the dq frame using (1). These commands are then compared against the measured real and reactive power, calculated using

$$\begin{cases} P = U_d I_d + U_q I_q \\ Q = U_q I_d - U_d I_q \end{cases} \cdots\cdots\cdots\cdots\cdots\cdots\cdots\cdots\cdots\cdots\cdots\cdots\cdots\cdots (2)$$

Where U_{dq} and I_{dq} are the measured grid voltages and currents in the dq frame. The power errors are then processed by standard PI regulators to generate commanded values for the current regulators in the next level down control system. The current controllers are conventional synchronous dq frame PI current regulators, with their PI gains set to the maximum possible stable values as will be discussed in Section C. The regulator outputs command the required modulation indices for the three phase inverter system, and are converted back to the stationary abc frame and fed into an asymmetrical regular sampled PWM modulator system to control the switching of each phase leg. Simulating the control systems in this way is well established in the literature as a technique that achieves a highly accurate simulation representation of real physical converter system operation, including in particular their high frequency dynamic and filter responses [17].

B.   Active Damping

Most leading edge DG converters use an LCL output filter system to get better switching frequency harmonic attenuation with reduced size filter components. These filters introduce a resonance peak into the plant frequency response which can cause resonant stability problems. Typically, either passive or active damping within the current regulator is required to avoid this instability [18, 19]. However, since passive damping increases the system losses, active damping by introducing a compensation term that is proportional to the capacitor current is the preferred approach.

International Journal for Research in Applied Science & Engineering Technology (IJRASET)

Fig. 3 shows a single loop representation of the d and q axis PI current regulators, modeled in the s-domain. The controller transfer function is given by
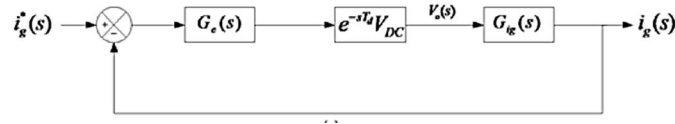

Fig.3 Single loop regulator.

$$G_s(s) = K_p \left(1 + \frac{1}{s\tau_i}\right) \dots\dots\dots (3)$$

With a proportional gain K_p and an integral time constant τi. From previous work [19] the LCL filter transfer function is

$$G_{ig}(s) = \frac{1}{sL_f} \frac{\gamma^2 LC}{(s^2 + W_{res}^2)} \dots\dots\dots\dots (4)$$

Where W_{res} is the resonance frequency given by

$$W_{res} = \sqrt{\frac{L_f + L_{fg}}{L_f L_{fg} C_f}} \dots\dots\dots\dots (5)$$

And
$$\gamma_{lc} = \sqrt{\frac{1}{L_f C_f}} \dots\dots\dots\dots\dots (6)$$

Note also that in this representation, the inverter has been modelled as a DC gain (V_{dc}), and a delay e^{-sT_d} has been included to represent the effects of controller sampling and PWM transport delay [17].

Fig. 3(b) shows how active damping can be introduced into this system, where the capacitor current (s) is used as a feedback signal, with a damping gain of K_d. The LCL filter transfer function is now split into two parts to model this arrangement, as
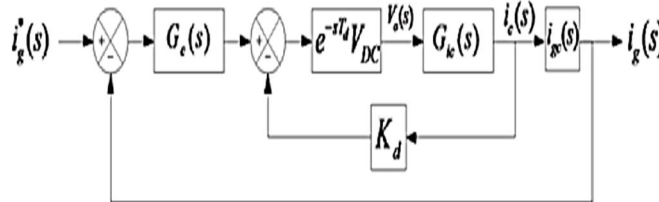

Fig.4 Dual loop regulator with capacitor current active damping.

$$G_{ic}(s) = \frac{1}{sL_f} \frac{s^2}{(s^2 + W_{res}^2)} \dots\dots\dots\dots (7)$$

$$\frac{i_{g(s)}}{i_{c(s)}} = i_{gc}(s) = \frac{\gamma_{LC}^2}{s^2} \dots\dots\dots\dots (8)$$

To ensure a worst case damping scenario, winding resistance and core loss of the inductors have been neglected in this modelling [17]. To analyses the frequency response of these two regulators, their open loop forward path expressions can be developed using (3)-(7), to achieve respectively.

$$H_{single\ loop}(s) = e^{-sT_d} V_{dc} G_c(s). G_{ig}(s) \dots\dots\dots (9)$$

$$H_{damped}(s) = \frac{V_{dc}G_{ic}(s)}{1+s\tau_i+K_dV_{dc}G_{ic}(s)} G_c(s)G_{ic}(s) .. (10)$$

Fig. 4 shows the corresponding frequency response of these two forward path transfer functions. With the single loop controller, there is an LCL filter resonance at 7.6 krad/sec, which introduces a sharp phase shift of −180° with a large magnitude peak. This is very likely to create an unstable operating condition for the controller, unless the PI gains are significantly limited. As can be seen, active damping essentially eliminates this resonance from the forward path, allowing the PI regulator gains to be substantially increased while still maintaining stable control.
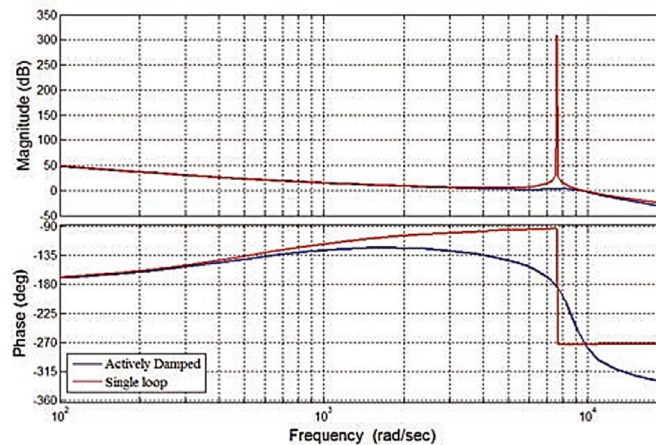

Fig. 5 Bode plot of the transfer function as defined in (8) and (9).

C. Current Controller Gains
The PI regulator gains are readily calculated using the methodology proposed in [17]. The maximum possible proportional gain is computed by

$$K_p = \frac{W_c(L_f+L_{fg})}{V_{dc}} \dots\dots\dots\dots\dots\dots\dots (11)$$

Where W_c is the cross over frequency calculated based on the desired phase margin $\emptyset_m$ and on the sampling period of

$T = {}^1/_{f_{samp}}$ According to

$$W_c = \frac{{}^\pi/_2 - \emptyset_m}{3^T/_2} \dots\dots\dots\dots\dots\dots\dots\dots (12)$$

If the phase contribution of resonant time constant τ_i is small at the crossover frequency, an appropriate value for the integral time constant can be obtained. Setting $\tau_i = 10/\omega c$ ensures an approximately 900 phase contribution at the crossover frequency, which gives the best possible frequency response without affecting the system stability. For the designed system with a resonant frequency of $f_{res} = 1.2094kHz$, sampling frequency of $f_{samp} = 10kHz$ and desired phase margin of $\emptyset_m = 45°$, the PI gains are calculated using these concepts as $Kp = 0.07315e^{-1}$ and $\tau_i = 0.00191s$.

D. Phase-Locked Loop (PLL)
The physical voltages and currents must always be measured in the stationary abc reference frame. Since the control structure is based in the synchronous dq frame, these quantities must be transformed before being used in the control loop calculations, and this requires continuous knowledge of the synchronous frame reference angle. This is measured using a phase locked loop as shown in Fig. 5. Essentially, the loop compares the angle of the quadrature axis voltage uq against zero, and forces the synchronous frame angle to the value that achieves this result using a standard PI regulator to process the error.

International Journal for Research in Applied Science & Engineering Technology (IJRASET)
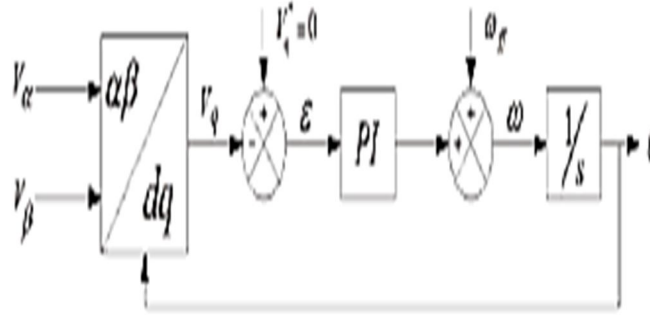

Fig .6 .Three-phase dq-PLL.

IV.   IMPLEMENTATION IN DIGSILENT

The modelling concepts presented above have been incorporated into the DigSILENT power system analysis package, starting with the basic power stage shown in Fig. 6. The inverter modelling is based on the "PWM converter" model with two DC connections. The DC connections are connected to a DC source which can represent the primary source of power. Then, to add the LCL filter, two "Common Impedances" are used for inverter-side and grid-side inductors, and a "Shunt/Filter C" is located in between these inductances for filter capacitance
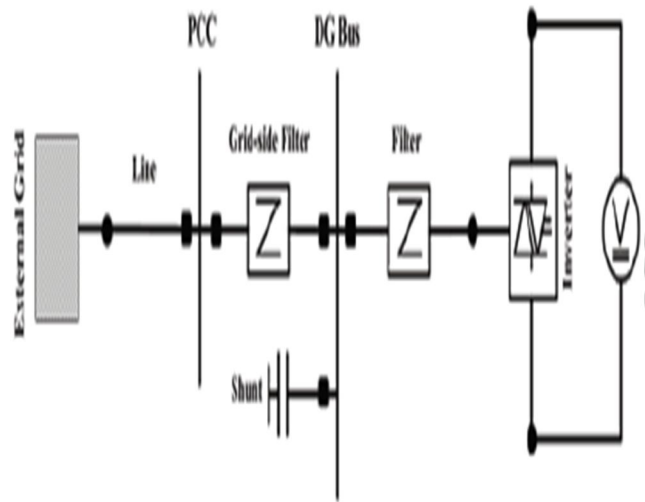

Fig .7 Power stage of the three-phase DG unit (single line Presentation)

A.   Block Definition

The required control system structures are now constructed to create the full model DG system. Fig. 7 shows the overall control structure of the DG unit as implemented in DigSILENT. The composite frame consists of voltage and current measurement blocks, sample and hold blocks, clock generator, dq transformation block, PLL system, power control frame (PQ), current control frame (Current) and finally the modulation indexes which are fed into the inverter modulator and power stage. The Current 3ph block and the Shunt Current block are the current measurement devices located at the grid side inductance/filter and on the filter capacitance respectively. To measure the PCC voltage the Voltage 3ph block is used. The ab2dq block includes the transformations required for the voltage and the current values to change their frame of reference to the dq rotating frame. The PQ block calculates the active and reactive powers and then generates the current references to be fed into the Current block. Finally, this block creates the modulation indexes for the Inverter block. The PLL block is added for the purpose of synchronization to the grid.

227

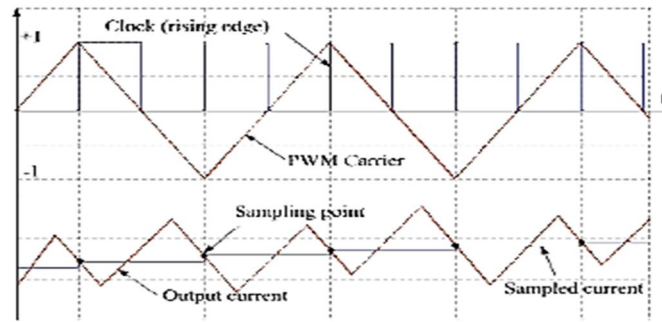# International Journal for Research in Applied Science & Engineering Technology (IJRASET)

Fig. 8 sampling procedure.

B. Sampling and Clock Generation

To account for digitalization, sampling blocks are used with the same clocking sequence for all of the sampling blocks. One important issue was to ensure that the power stage voltages and currents were measured exactly at the transition point of each half carrier period (synchronous sampling) as shown in Fig. 8, to avoid sampling the switching ripple effects. This required the inclusion of the sample and hold model (ElmSamp) into the variable measurement blocks, to keep the measured quantities constant over each half carrier period. The sampling frequency is set to twice the switching frequency of the inverter. The sampling is done at the rising edge of the clock. Therefore, the clock is defined in a fashion that the rising edge of the clock is located exactly at the minimum and maximum points of the carrier. This eliminates measurement of the switching ripple current.

C. Power Control Block

The implementation of power control in DigSILENT is shown in Fig. 9. This is the control block identified as the PQ block in Fig. 7. It begins by calculating the actual real and reactive power for the converter, using the measured (dq frame) voltages and currents. A PI regulator then compares the power set points against these actual powers, and uses the errors to command the required currents to achieve the commanded real and reactive power. A particular benefit of this approach is that commanded step changes in power flow translate to ramp changes in the commanded current because of the action of the PI controller, which reduces transients injected into the distribution system from the converter.

D. Current Control Block

Fig. 10 shows that how current regulation is implemented in DigSILENT. The reference currents are provided by the PQ block. The mathematics of the modelling of the current regulator have already been explained in Section III part B and C. In order to apply active damping, the measured capacitor currents are fed into this block as well. These currents are added as additional feedback signals after the PI regulators, with a damping gain of Kd. The outputs of the current controllers are the commanded dq frame voltages that are required to be produced by the converter power stage. They are converted back into stationary frame αβ commands as the output of the control block, to suit the DigSILENT power stage representation of the converter system shown in Fig 6.
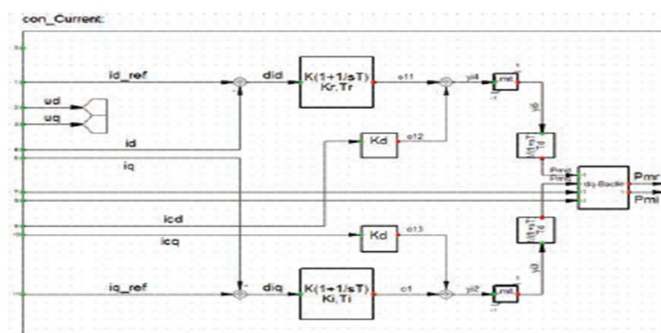
V. SIMULATION MODELS AND RESULTS

Fig 9 current control block

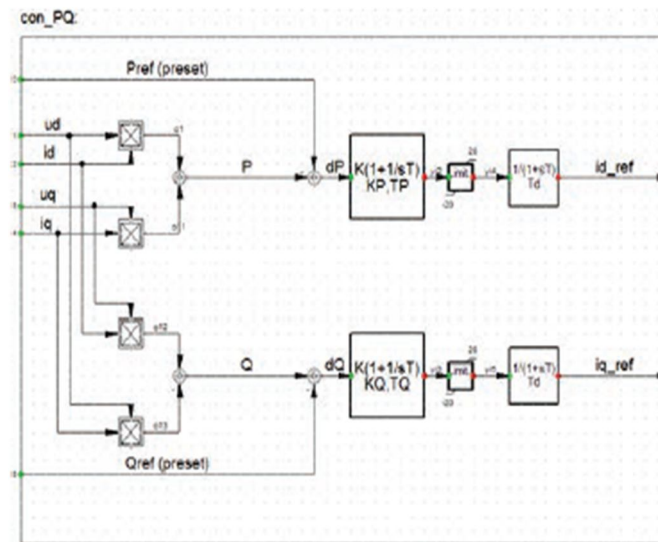# International Journal for Research in Applied Science & Engineering Technology (IJRASET)
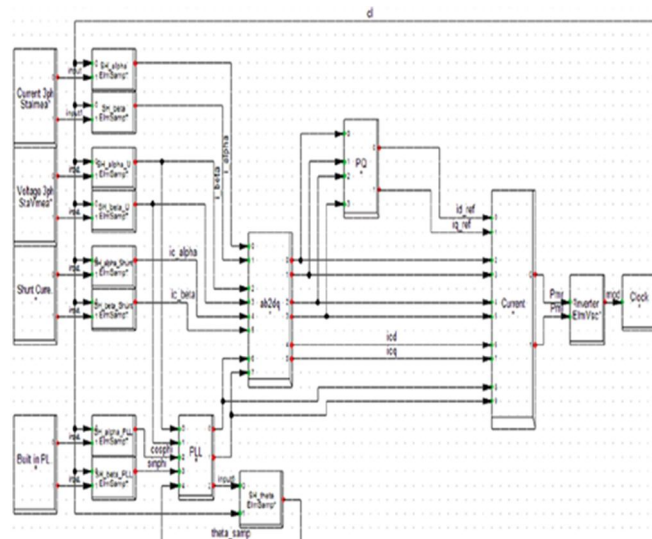

Fig 10 PQ control block

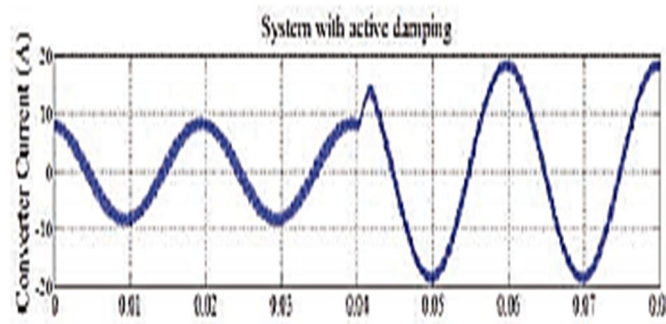Fig. 11 DG converter controller implemented in DigSILENT

Fig.12 Phase A Current with step change in Power Reference Converter side

International Journal for Research in Applied Science & Engineering Technology (IJRASET)
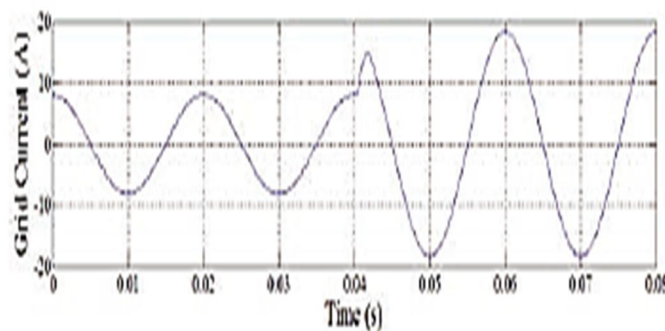

Fig 13 Phase A Current with step change in Power Reference Grid side.

It shows the simulated performance of the DG system, presenting the converter side current (upper trace) and the grid side current (lower trace). The converter side current has an obvious switching ripple component, while this ripple is not present in the grid side current. This demonstrates the very effective response of the LCL filter in preventing the inevitable converter side switching harmonics from injecting into the grid network. Fig. 11 also illustrates the excellent transient step response achieved for the regulator where the current increases magnitude rapidly and smoothly as the commanded power reference changes, with no sign of overshoot or transient instability.

DigSILENT is a power system analysis tool that is primarily used for electrical network planning and operation investigation requires it to implement a more detailed simulation of the DG inverter system, including a quite precise representation of the inverter switching processes.
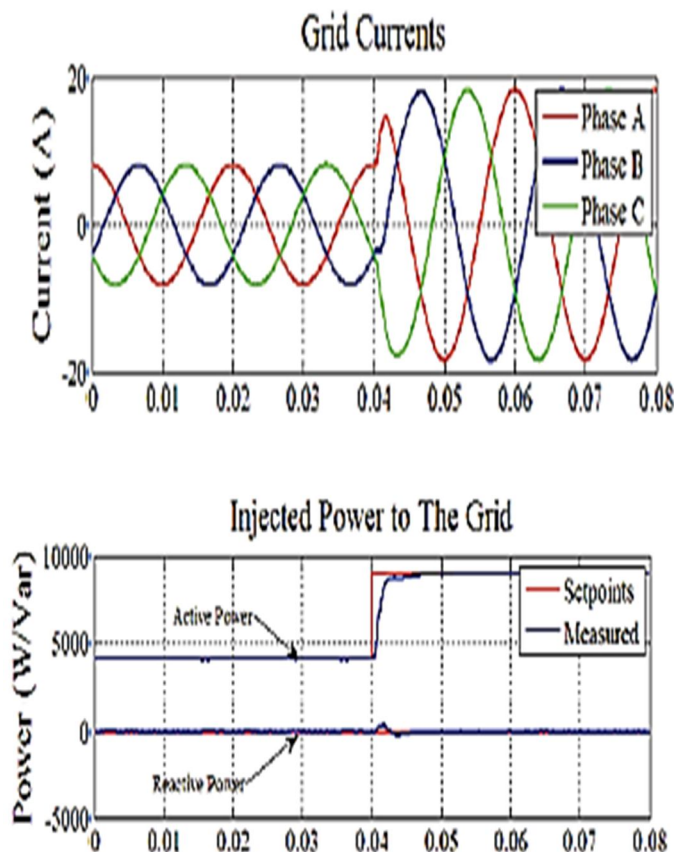
230

International Journal for Research in Applied Science & Engineering Technology (IJRASET)
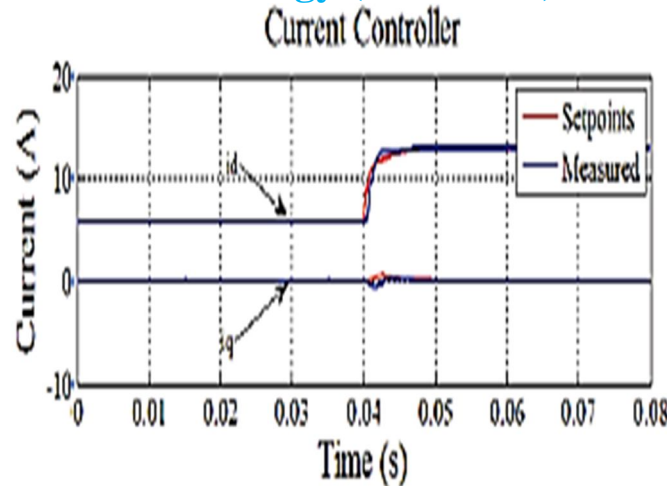

Fig 14 grid currents and injected power to grid current controller wave forms

For the current regulator, the commanded active power corresponds to the direct axis current, while the commanded reactive power corresponds to the quadrature axis current. Hence the real power change causes a step in the d-axis current (id), while the q-axis current component ( ) remains at zero because there is no reactive power injection into the grid.

A.   Micro grid

To study a multi-bus multi-DG system, a 20-bus micro grid was constructed incorporating distributed generation as shown in Fig. 15. For this network, a DG unit modelled using the approach just presented was connected to each bus, together with a local PQ load on the bus. The total penetration of the DG units was limited to not exceed 40% of total installed load, with the remainder of the micro grid power being supplied by the synchronous generator at the "Station" bus, as shown in Fig. 14. To prevent switching harmonic coherency between the inverters, the switching frequency of each inverter was randomly set with different values between 5 kHz to 6 kHz.
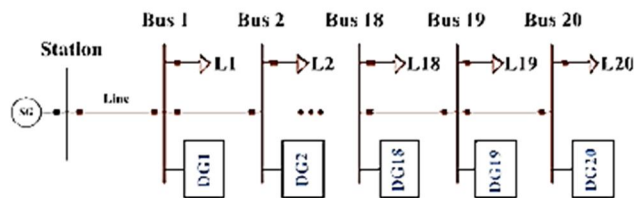

Fig 15 20 bus micro grid

The synchronous generator output powers are presented in Fig. 16. It is shown that as could be anticipated, at 0.05 s, when reactive power generation of DG units changes, the reactive power injected by the synchronous generator decreases while its active power slightly increases because of the changes in losses in the network. To illustrate the impact of this increase in reactive power generation along the distribution feeder, the voltage magnitude is shown in Fig. 17 for two buses along the feeder, one at the synchronous generator terminal, and one for bus #20 at the end of the feeder. As the reactive power injection increases from the distributed generation system, the voltage profile along the feeder increases, with minimal overshoot and no sign of dynamic instability during the transient event.

International Journal for Research in Applied Science & Engineering Technology (IJRASET)
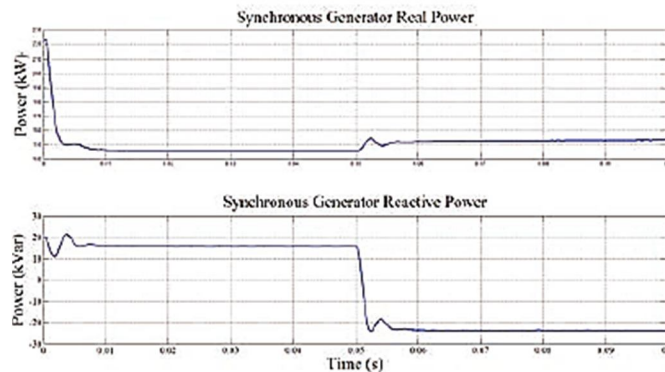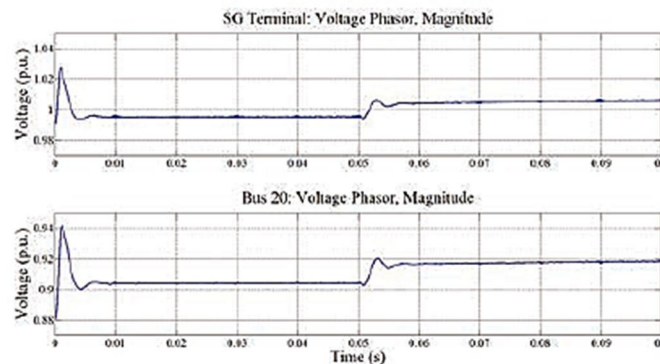

Fig. 16 synchronous generator powers

Fig 17 voltage profile along the feeder

VI.   CONCLUSION

This paper has presented a modelling strategy for DG converters that is suitable for studying the large scale integration of DG systems into the electrical grid. The model combines the fundamental inverter switching modulation process with a leading edge current regulator and higher level real and reactive power controllers, to create a detailed representation that fully describes the inverter steady state and transient responses to grid connection events. The inverter connects to the grid via an LCL filter, and the controller gains are set to their maximum possible values, using a deterministic calculation that is based on the filter components and modulation/control sampling and transport delays. Power electronic converter modelling package, to confirm the validity of the approach. The result is a model that is sufficiently accurate to match known experimental behavior of these types of converter, and is computationally efficient enough to allow large numbers of converter systems to be simulated in a large scale grid network with confidence that the results are a realistic reflection of a real physical system.

REFERENCES

[1] R. H. Lasseter, "Smart Distribution: Coupled Microgrids," Proceedings of the IEEE, vol. 99, pp. 1074-1082, 2011.
[2] "Smart Grid: An Introduction U.S. Department of Energy," 2009.
[3] R. H. Lasseter and P. Paigi, "Microgrid: a conceptual solution," in Power Electronics Specialists Conference, 2004. PESC 04. 2004 IEEE 35th Annual, 2004, pp. 4285-4290 Vol.6.
[4] M. A. Zamani, A. Yazdani, and T. S. Sidhu, "A Control Strategy for Enhanced Operation of Inverter-Based Microgrids Under Transient Disturbances and Network Faults," Power Delivery, IEEE Transactions on, vol. 27, pp. 1737-1747, 2012.
[5] A. Kahrobaeian and Y. A. R. I. Mohamed, "Interactive Distributed Generation Interface for Flexible Micro-Grid Operation in Smart Distribution Systems," Sustainable Energy, IEEE Transactions on, vol. 3, pp. 295-305, 2012.
[6] R. Tonkoski, D. Turcotte, and T. H. M. El-Fouly, "Impact of High PV Penetration on Voltage Profiles in Residential Neighborhoods," Sustainable Energy, IEEE Transactions on, vol. 3, pp. 518-527, 2012.

International Journal for Research in Applied Science & Engineering Technology (IJRASET)

[7] M. E. Baran, H. Hooshyar, S. Zhan, and A. Huang, "Accommodating High PV Penetration on Distribution Feeders," Smart Grid, IEEE Transactions on, vol. 3, pp. 1039-1046, 2012.

[8] S. A. Pourmousavi, A. S. Cifala, and M. H. Nehrir, "Impact of high penetration of PV generation on frequency and voltage in a distribution feeder," in North American Power Symposium (NAPS), 2012, 2012, pp. 1-8.

[9] A. K. Srivastava, A. A. Kumar, and N. N. Schulz, "Impact of Distributed Generations With Energy Storage Devices on the Electric Grid," Systems Journal, IEEE, vol. 6, pp. 110-117, 2012.

[10] W. Fei, J. L. Duarte, M. A. M. Hendrix, and P. F. Ribeiro, "Modeling and Analysis of Grid Harmonic Distortion Impact of Aggregated DG Inverters," Power Electronics, IEEE Transactions on, vol. 26, pp. 786-797, 2011.

[11] M. Liserre, R. Teodorescu, and F. Blaabjerg, "Multiple harmonics control for three-phase grid converter systems with the use of PI-RES current controller in a rotating frame," Power Electronics, IEEE Transactions on, vol. 21, pp. 836-841, 2006.

[12] J. H. R. Enslin and P. J. M. Heskes, "Harmonic interaction between a large number of distributed power inverters and the distribution network," Power Electronics, IEEE Transactions on, vol. 19, pp. 1586-1593, 2004.

[13] W. Xiongfei, F. Blaabjerg, and C. Zhe, "A current controller of gridconnected converter for harmonic damping in a distribution network," in Electrical Machines and Systems (ICEMS), 2011 International Conference on, 2011, pp. 1-6.

[14] J. Desmet, C. Debruyne, J. Vanalme, and L. Vandevelde, "Power injection by distributed generation and the influence of harmonic load conditions," in Power and Energy Society General Meeting, 2010 IEEE, 2010, pp. 1-6.

[15] R. Teodorescu, F. Blaabjerg, U. Borup, and M. Liserre, "A new control structure for grid-connected LCL PV inverters with zero steady-state error and selective harmonic compensation," in Applied Power Electronics Conference and Exposition, 2004. APEC '04. Nineteenth Annual IEEE, 2004, pp. 580-586 Vol.1.

[16] DigSILENT PowerFactory 14, User's Manual.

[17] D. G. Holmes, T. A. Lipo, B. P. McGrath, and W. Y. Kong, "Optimized Design of Stationary Frame Three Phase AC Current Regulators," Power Electronics, IEEE Transactions on, vol. 24, pp. 2417-2426, 2009.

[18] J. Dannehl, C. Wessels, and F. W. Fuchs, "Limitations of Voltage-Oriented PI Current Control of Grid-Connected PWM Rectifiers With LCL Filters," Industrial Electronics, IEEE Transactions on, vol. 56, pp. 380-388, 2009.

[19] J. Dannehl, F. W. Fuchs, S. Hansen, and P. B. Thogersen, "Investigation of active damping approaches for PI-based current control of grid-connected PWM converters with LCL filters," in Energy Conversion Congress and Exposition, 2009. ECCE 2009. IEEE, 2009, pp. 2998-3005.2

VenkateswaraReddy.G received the B.Tech degree in Electrical and Electronic Engineering from Jawaharlal Nehru technological university Kakinada, India in 2012. And he is currently working a post graduate fellow in the Lakkireddy Balireddy College of Engineering, India, his research interests include power electronics and drives and renewable energy power conversion systems.

Chandrakala.Batti received the B. Tech degree in Electrical and Electronics Engineering from JawaharlalNehru technological university Hyderabad in 2007. And she received the M. Tech degree in power electronics from Jawaharlal Nehru Technological University Anatnapur in 2011. From 2007 to 2008 she was an assistant professor in sri sai institute of technology & science, India. She currently works as assistant professor in lakkireddy Balireddy College of Engineering from 2011. She published a 4 peer reviewed technical papers. Her research interests in power electronics and drives and renewable energy systems.

INTERNATIONAL JOURNAL FOR RESEARCH

IN APPLIED SCIENCE & ENGINEERING TECHNOLOGY

Call : 08813907089 (24*7 Support on Whatsapp)